Estimating floor spectra in multiple degree of freedom systems

Paolo M Calvi[*1] and Timothy J Sullivan[2a]

[1]*Department of Civil Engineering, University of Toronto, 35 St. George Street, Toronto, ON M5S 1A4, Canada*
[2]*Department of Civil Engineering and Architecture, Universita' degli Studi di Pavia,*
Via Ferrata 1, 27100, Pavia, Italy

Abstract. As the desire for high performance buildings increases, it is increasingly evident that engineers require reliable methods for the estimation of seismic demands on both structural and non-structural components. To this extent, improved tools for the prediction of floor spectra would assist in the assessment of acceleration sensitive non-structural and secondary components. Recently, a new procedure was successfully developed and tested for the simplified construction of floor spectra, at various levels of elastic damping, atop single-degree-of-freedom structures. This paper extends the methodology to multi-degree-of-freedom (MDOF) supporting systems responding in the elastic range, proposing a simplified modal combination approach for floor spectra over upper storeys and accounting for the limited filtering of the ground motion input that occurs over lower storeys. The procedure is tested numerically by comparing predictions with floor spectra obtained from time-history analyses of RC wall structures of 2- to 20-storeys in height. Results demonstrate that the method performs well for MDOF systems responding in the elastic range. Future research should further develop the approach to permit the prediction of floor spectra in MDOF systems that respond in the inelastic range.

Keywords: floor spectra; non-structural; secondary structural elements; floor accelerations

1. Introduction

As demands for performance based earthquake engineering increase, there is an increasing awareness that two of the most useful engineering demand parameters are storey drift and floor acceleration. With the continuing development of displacement-based design (Priestley *et al*. 2007, Garcia *et al*. 2010, Maley *et al*. 2010, Sullivan 2011, Sullivan 2013) and assessment (Welch *et al*. 2014), one could argue that engineers already possess a range of tools for simplified assessment of storey drift demands. For what regards accelerations, however, there still appears to be an opportunity to develop simplified tools for the estimation of floor acceleration demands. Moreover, one could argue that controlling damage to acceleration sensitive non-structural elements requires knowledge of floor acceleration response spectra and not just of peak floor acceleration demands, since a floor spectrum provides valuable indications of demands at different periods of vibration so that element-specific seismic assessment or design can be undertaken. As shown in Fig. 1, it is

---

∗Corresponding author, Ph.D. candidate, E-mail: paolo.calvi@mail.utoronto.ca
[a]Assistant Professor, E-mail: timothy.sullivan@unipv.it

clear that floor spectra should be expected to differ at each level of a structure since the arriving ground motion will be filtered by the dynamic response of the structure, such that (for example) roof level response spectra can differ significantly from ground level response spectra, both in shape and magnitude.

Current codes provide approximate methods for the estimation of acceleration demands on components at different levels of a building. However, several authors (Mondal and Jain 2005, Oropeza *et al.* 2010, Sullivan *et al.* 2013, amongst others) have shown that existing code approaches are not reliable and subsequently there have been many alternative approaches proposed in the literature for estimation of floor spectra (Biggs 1971, Vanmarcke 1977, Singh 1980, Igusa and Der Kiureghian 1985, Villaverde 2004, Taghavi and Miranda 2006, Kumari and Gupta 2007, Menon and Magenes 2008, Sullivan *et al.* 2013 amongst others). Of these methods, the approach of Taghavi and Miranda (2006) appears to be promising, but does require relatively advanced analysis capabilities. Furthermore, only the earlier approaches provide some guidance for the construction of floor spectra at different levels of elastic damping and attempt to make explicit but simple evaluation of the effects of higher modes of vibration. In particular, the method proposed by Biggs (1971) comprises a relatively simple means of constructing floor response spectra accounting for both aspects. Nevertheless, the approach by Biggs strongly relies on a series of empirical coefficients that were calibrated and corroborated only by a small number of numerical analyses, which means it is of limited accuracy and applicability in practice, as will be illustrated later in this paper.

To address such limitations with existing methods, Sullivan *et al.* (2013) recently proposed a new method for the estimation of floor spectra which uses a mechanics based approach to set the spectral shape and an empirical relationship to set the magnitude of the response spectrum.The method was shown to predict the floor spectra atop SDOF systems well, for various levels of elastic damping and even when the supporting structure behaved non-linearly. The procedure has not yet been extended, however, to the case of MDOF supporting systems.

Given these observations, this paper extends on the work of Sullivan *et al.* (2013) to present a new, simple approach for the prediction of acceleration spectra for the design of secondary structural and non-structural elements in elastic MDOF supporting structures. The methodology utilizes results of modal analyses of the supporting structure together with an empirical relationship to set the peak spectral acceleration demands as a function of the damping of the supported element. Results of time-history analyses of case study structures will be used to illustrate that the new procedure appears to work well.

2. Relevance of higher modes of vibration on floor accelerations

When dealing with seismic design of structures, the most simplified procedure allowed by most codes is known as the "equivalent lateral force method". Without entering into the contradictions inherent in this and other force based design approaches, the validity of this method relies on the assumption that the building under investigation can be well represented by its first mode of vibration.

Even though the effects of higher modes can often be neglected from the point of view of displacement control, the floor accelerations that are produced by higher modes of vibration can be very significant. It is common belief that a relatively short and regular building can be accurately

Table 1 Elastic 2DOF case study structure properties

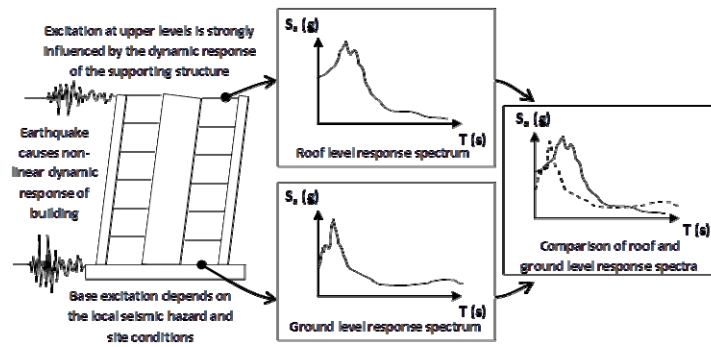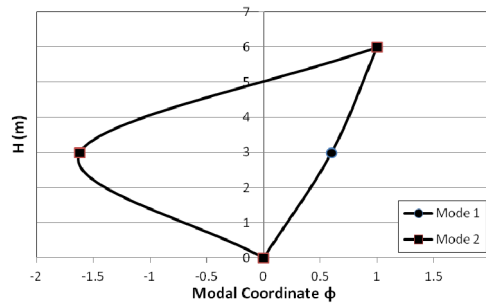| Floor	Lateral stiffness (kN/m)	Mass (ton)	Damping ratio ξ (%)	T_1 (s)	T_2 (s)
1	100	0.25	5		0.19
2	100	0.25	5	0.5	

Fig.1 Illustration of roof and ground level response spectra (adapted from Sullivan *et al*. 2013)

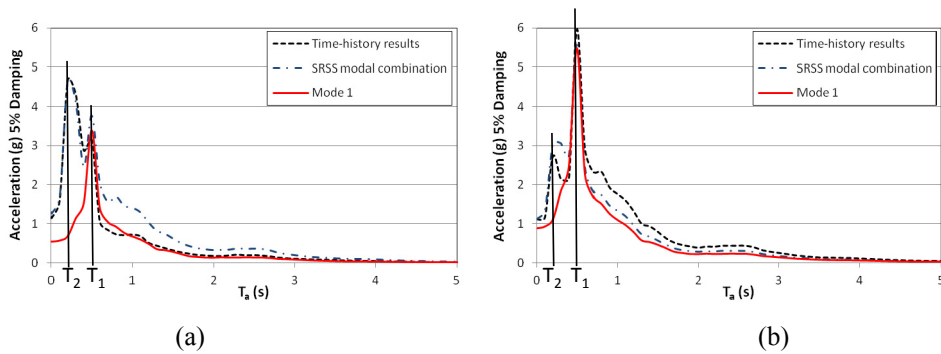Fig. 2 Mode shapes of the 2DOF case study structure

| (a) | (b) |

Fig. 3 First floor response spectra (left) and roof level response spectra (right). The plots are relative to the ground motion "Alkion" (Table 4) and the properties of the supporting structures are listed in Table 1

represented through the first mode of vibration or through an approximation of the first mode itself. However, it should be recognized that the floor accelerations induced by the higher modes can be very large even in a 2-storey building, and should not be neglected when assembling floor response spectra.

To illustrate the point made above, analysis results for a simple 2 degree-of-freedom (DOF) structure responding in the elastic range are briefly presented here. The properties of the structure are listed in Table 1. The floor masses and floor stiffness are constant over the height of the structure. The system studied does not represent any specific practical structure as the aim is only to illustrate that, even for a very simple case, higher modes of vibration can play a crucial role.

However, note that the first mode period of 0.5s could be considered reasonable for a 2-storey moment-resisting frame building.

The system is analyzed performing an exact modal analysis. Mass and stiffness matrices as well as damping matrices are classically constructed (see Chopra 2000) and damping is idealized in line with the classic Rayleigh model (therefore proportional to mass and stiffness). Exploiting the orthogonality of modes, the contribution of each mode is isolated, and the modal acceleration history is computed at each floor multiplying the individual modal accelerations by the appropriate modal coordinates. The global absolute floor acceleration is finally obtained summing the contribution of each mode. Once the absolute floor acceleration is known at each location, the relative floor response spectra are evaluated in line with Newmark's classic method (see Chopra 2000). The mode shapes obtained from the analyses are indicated in Fig. 2 and the periods of vibration are shown in Table 1.

Results obtained from this process for the 2-storey structure subject to the Alkion accelerogram (for details see Table 4) are summarized in Fig. 3. For comparison reasons, acceleration spectra associated with the individual modes at both the first and second floor are also constructed as separate curves and combined according to an SRSS method.

Examining Fig. 3, it can be observed that the first mode spectrum is unable to properly reproduce the floor response spectra, particularly at the first floor level. At this location, the effects of the second mode induce an acceleration peak which is greater than that associated with the first mode. A first mode approximation provides therefore an extremely inappropriate evaluation of the first floor acceleration response spectrum. Less concerning is the situation with respect to the roof level. The influence of the second mode is in fact milder (as can be expected referring to the mode shapes in Fig. 2) and the first mode spectrum better captures the actual shape of the spectrum. Nevertheless, the peak associated with the second mode is neglected and a non-conservative estimate of the acceleration felt by components characterized with periods of vibration in the vicinity of T_2 still results. A much better representation of the actual curves is achieved if both the spectra associated with the first and second mode are constructed and combined to provide an approximate solution.

The findings of this section indicate that the higher modes (and in this case, the second mode of vibration) can produce large floor acceleration spikes, even in a simple 2DOF regular elastic system. The contributions of higher modes influence the shape and the intensity of floor response spectra significantly. As a consequence, neglecting the effects of the higher modes of vibration when constructing acceleration response spectra at different levels of a building, can lead to inaccurate evaluation of the risks associated with components characterized by periods of vibration in the vicinity of higher mode periods.
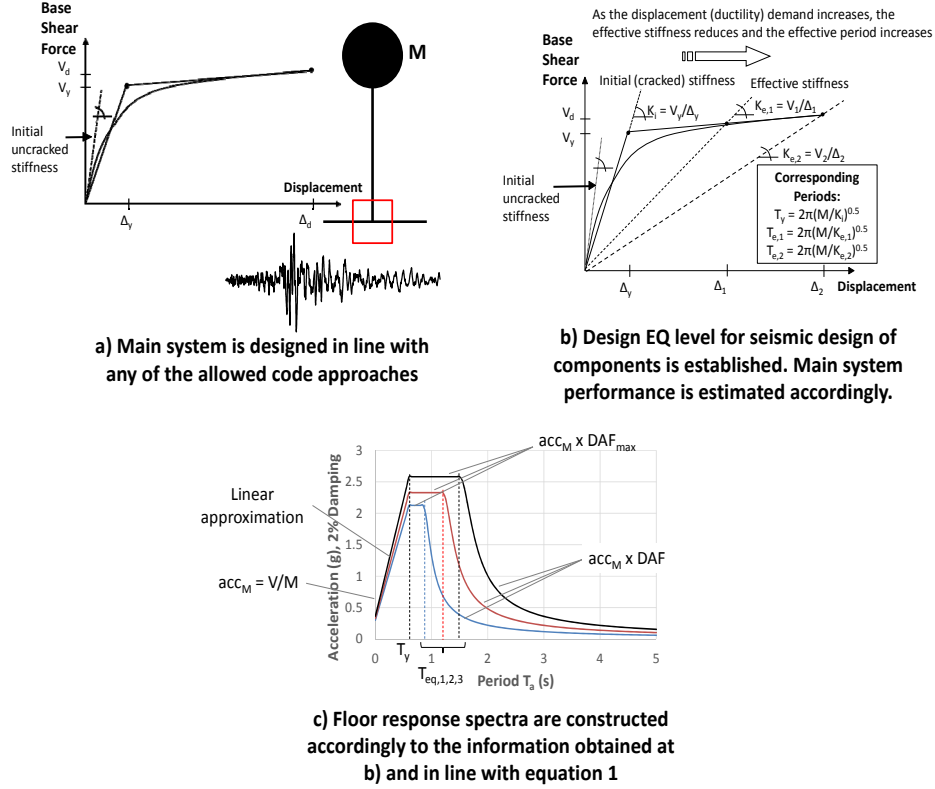
a) Main system is designed in line with any of the allowed code approaches

b) Design EQ level for seismic design of components is established. Main system performance is estimated accordingly.

c) Floor response spectra are constructed accordingly to the information obtained at b) and in line with equation 1

Fig. 4 Overview of floor spectra construction procedure for SDF elastic and inelastic systems

3. Towards a simplified means of constructing floor spectra in MDOF systems

3.1 Response spectra atop SDOF systems

Before addressing MDOF systems, this section reviews the original method proposed by Sullivan *et al*. (2013) for floor spectra atop SDOF systems, making reference to Fig. 4. As shown in Fig. 4a, the main structural system is first designed and analyzed. The effective period at the expected response point is then identified as shown in Fig. 4b. With knowledge of the initial and effective period of the supporting structure, as well as the maximum acceleration expected for the seismic mass, floor spectra are then constructed (Fig. 4c) at different elastic damping values using the concept of an apparent dynamic amplification factor.

The concept of an apparent dynamic amplification factor was introduced for floor spectra by Sullivan *et al*. (2013) in recognition of the fact that the dynamic response will be dependent on excitation characteristics and earthquakes impose neither harmonic excitation nor clearly defined impulse loading. An empirical expression for the dynamic amplification factor was therefore proposed and successfully validated using the results of non-linear time-history (NLTH) analyses of SDOF systems subject to a large suite of earthquake ground motions. A new series of empirical equations were then proposed to predict floor spectra on SDOF supporting structures:

$$a_m = \frac{T}{T_y}\left[a_{max}(DAF_{max}-1)\right]+a_{max} \quad T < T_y$$

$$a_m = a_{max}DAF_{max} \quad T_y \leq T < T_e \tag{1}$$

$$a_m = a_{max}DAF \quad T \geq T_e$$

where a_m is the acceleration spectral coordinate for a supported element of period T, a_{max} is the maximum acceleration of the mass of the supporting structure (obtained for SDOF systems as the minimum of either the structure's lateral resistance divided by its seismic mass or from a ground level response spectrum), T_y is the natural (elastic) period of the supporting structure, T_e is the effective period of the supporting structure, DAF is the empirical dynamic amplification factor (i.e. the ratio of the acceleration, a_m, felt by a component with a given period of vibration and the maximum acceleration of the floor, a_{max}) from Eq. (2) with $\beta = T_e/T$, and DAF_{max} is the maximum expected dynamic amplification obtained from Eq. (3).

$$DAF = \frac{1}{\sqrt{\left(1-\frac{1}{\beta}\right)^2 + \xi}} \tag{2}$$

$$DAF_{max} = \frac{1}{\xi^{0.5}} \tag{3}$$

where ξ is the level of elastic damping that characterizes the supported component.
This empirical approach of Sullivan *et al*. (2013) accounts for different frequencies and inelasticity of the supporting structure to define the shape of the floor spectra and uses the elastic damping of the supported element in order to define the magnitude of the floor spectra. The results of NLTH analyses of a series of SDOF supporting structures subject to earthquake motions of varying intensity have indicated that the new methodology is very promising. In addition, the method can be efficiently employed whether the main structure responds in the elastic or inelastic range. However, the approach is currently limited to response spectra atop SDOF systems and therefore the next sections will illustrate how to the approach can be extended for use with MDOF supporting systems.

3.2 Extending the procedure to MDOF supporting systems

One of the most commonly adopted means of designing structures for earthquakes in line with code legislation is to use response-spectrum analysis, also referred to as multi-modal analysis, in order to obtain estimates of structural response both in terms of design forces and displacements. The first step of the procedure is to perform eigen-value analysis of the structure with a given mass and elastic stiffness in order to identify its modal characteristics. The characteristics of particular importance are modal periods and modal shapes. The modal periods are used together with the design acceleration spectrum to read off acceleration coefficients for each mode. The mode shapes furnish the mass excited by each mode, which is then multiplied by the acceleration coefficient to give individual modal base shears. By distributing the base shear for each mode up the height of the structure as a set of equivalent lateral forces (proportional to the mode shape and mass

a) Eigen-value analysis of elastic structure
to give mode shapes and periods

b) Spectral analysis to obtain acceleration
of individual modal components

c) Distribution of individual modal components
of the acceleration along the height

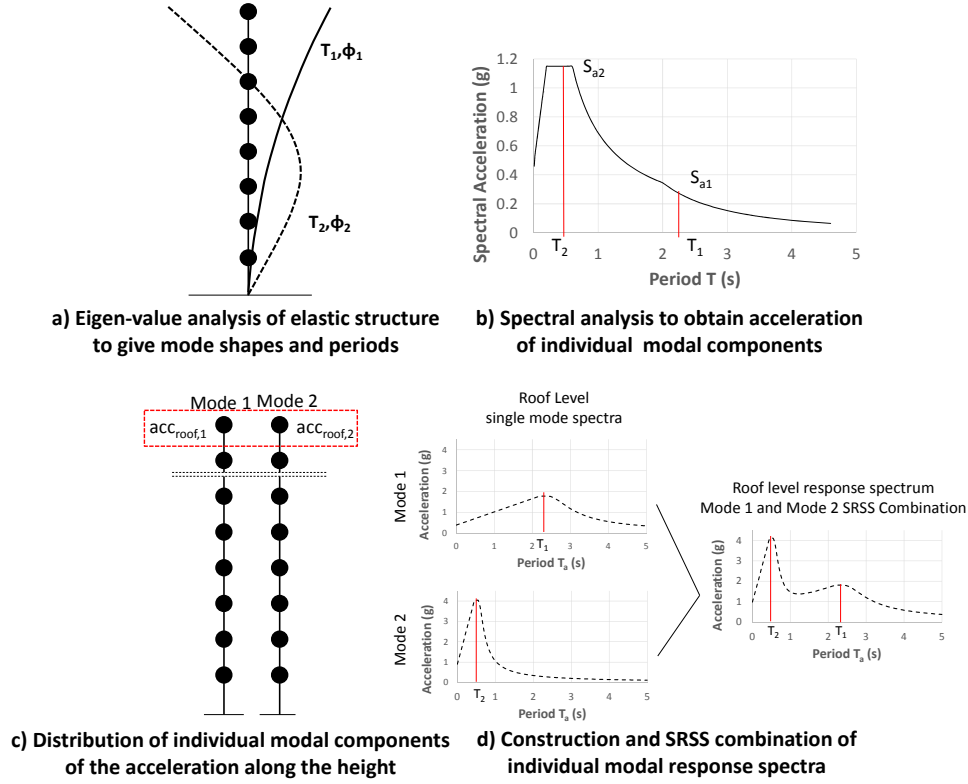d) Construction and SRSS combination of
individual modal response spectra

Fig. 5 Overview of floor spectra construction procedure for upper storeys of MDOF elastic systems

distribution), the elastic-response is obtained for each mode. These components are then combined in accordance with established modal combination rules, such as SRSS or CQC (see Chopra, 2000), to provide design forces and displacements associated with elastic response.

The modal response spectrum can be useful for the design of the main structural system but because non-structural elements are not typically modeled when undertaking eigen-value analyses, the approach does not identify relevant demands for their design and instead, can only be used to identify peak accelerations of the floors themselves. However, it does provide useful information on relative modal components and furthermore, because of the orthogonality of modes, each modal component can be assessed separately and then combined. With this in mind, it is proposed that the procedure of Sullivan *et al.* (2013) be extended to MDOF supporting systems by using the modal procedure proposed in Fig. 5.

As shown in Fig. 5a, the method starts with the dynamic analysis of the main structure. Once the modal properties (periods of vibration and mode shapes) are known, the peak floor acceleration due to each of the modes being considered is obtained (Fig. 5b) at each level (Fig. 5c). At this point, it is proposed that floor response spectra associated with each mode can be constructed according to Eq. (1), following the approach described in Section 3.1, and subsequently combined in line with SRSS method or analogous (Fig. 5d) to obtain the final floor spectra over the upper levels of the building.

While the modal procedure outlined in Fig. 5 is proposed for the upper storeys of MDOF systems, adjustment is required over the lower levels. This is because in order for an acceleration signal to be filtered, it is necessary that the natural frequency of the filter is lower than the frequency of the signal as otherwise, the amplitude of the transfer function is constant and equal to one. This in turn suggests that acceleration demands in the short to medium period range will only be filtered by the first few modes of vibration. Acceleration demands associated with higher modes, however, could be significant in the lower levels and are not likely to be filtered, transferring instead the ground motion acceleration demands unaltered. This hypothesis appears to be supported by results obtained by Rodriguez *et al*. (2002) and Lopez-Garcia *et al*. (2008) who were investigating floor acceleration related issues in MDOF systems and by Pennucci *et al*. (2011), who presented an extensive discussion on the dynamic response of RC wall systems. Rodriguez *et al*. (2002) report that first floor accelerations in the lower storeys of a structure are strongly influenced by the horizontal ground acceleration but did not propose reasons for this. Pennucci *et al*. (2011) suggested that the discrepancy between LTH and RSA is likely due to the modal combination rule used to add the contribution of the various modes. Given that these observations generally support the hypothesis of limited higher mode filtering, it is proposed that floor spectra over the lower levels of a MDOF supporting structure be obtained as a curve that envelopes the floor spectra constructed from the new modal approach (just described in Fig. 5) and the ground level response spectrum.

Overall, the proposed procedure for MDOF systems is therefore a relatively simple extension of the approach proposed by Sullivan *et al*. (2013). To this extent, it is clear that a reasonable estimate of floor spectra in line with the proposed procedure can only be achieved if the maximum dynamic amplification of the peak floor acceleration (DAF_{max} in Eq. (1)) is well approximated. This coefficient is of crucial importance in order to capture the floor spectra peak intensities and will be examined in some detail in the next section.

3.3 Dynamic amplification of the peak floor acceleration

To properly study the maximum apparent dynamic amplification (i.e., calibrating Eq. (3)) for the maximum floor acceleration in MDOF structures, it is necessary to separate the effects of the various modes. In doing so, the seismically excited MDOF system is transformed into several equivalent SDOF systems. The acceleration filtered by the equivalent SDOF systems is then used to construct the floor response spectrum relative to the specific mode under consideration. Note that for a given mode of vibration, amplification factors are the same over all floors and demands should only vary in proportion to the modal coordinate of the specific floor. Investigating the apparent dynamic amplification of the floor acceleration for each mode separately, is therefore analogous to a study of the same phenomenon adopting SDOF elastic systems characterized by different periods of vibration as supporting structures. Such an investigation was conducted by Sullivan *et al*. (2013). For preliminary design purposes, it was concluded that the dynamic amplification can be considered to be independent of the properties of the SDOF supporting system and it was proposed that the maximum dynamic amplification of the floor acceleration could be set only as a function of the inherent damping of the component to be designed. Larger data dispersion appeared for lightly damped components, while little scatter was observed for greater damping values.

Even though the results presented in Sullivan *et al*. (2013) were satisfactory overall, a minor

adjustment of the proposed function is made as part of the present work. As pointed out by Menon and Magenes (2008) amongst others, stiff supporting structures tend to provide little filtering of the ground motion. For instance, the acceleration recorded at the top of an infinitely stiff SDOF supporting structure would look exactly like the ground motion itself. The average floor response spectra relative to such a case and constructed using the records listed in Table 4, are shown in Fig. 6b for different levels of damping. One should appreciate that the maximum dynamic amplification of the peak floor acceleration is still damping dependent, but that it would be significantly overestimated by Eq. (2). The stiffest structure considered in the study by Sullivan *et al.* (2013) was characterized by a period of vibration of 0.3 seconds. Two additional systems characterized by periods of vibration of 0.1 and 0.2 seconds respectively and undergoing the same set of ground motions, are added to the database as part of the present study.

Based on the new results and the point made above about short periods, an alternative formulation for Eq. (1) is proposed as Eq. (4):

$$\begin{cases} DAF_{max} = \dfrac{C_1}{\left(C_3 - \dfrac{T_y}{T_B}\right)\xi C_2} & if\ 0 \le T_a < T_B \\[4mm] DAF_{max} = \dfrac{C_1}{\xi C_2} & if\ T_a \ge T_B \end{cases} \tag{4}$$

where $C_1 = 1.0$, $C_2 = 0.5$, $C_3 = 1.79$ and $T_B = 0.3s$. Note that C_3 has been set so that the amplification at $T_y = 0s$ is equal to 2.5 when elastic damping is 5%. The results shown in Fig. 6(a) indicate that Eq. (4) performs well.

The influence of ground motion characteristics on peak floor acceleration demands has also been investigated as in the previous study by Sullivan *et al.* (2013). Apparent dynamic amplifications have been obtained for both long-duration records and records with velocity-pulses. The results suggest that dynamic amplification factors for long duration accelerograms may be similar to those obtained for normal duration records and that dynamic amplification factors may need to be magnified to account for the possibility of velocity pulses from near-source earthquake events. Nevertheless, at this stage, Eq. (4) is considered to be sufficiently accurate to be employed with some confidence in practice.

The approach of constructing acceleration floor spectra by amplifying either the peak ground acceleration or the peak floor acceleration has also been advocated in the past. Biggs (1971) derived empirical dynamic amplification coefficients obtained fromtime-history analyses of a single 2 DOF case study structure, subjected to four different ground motions. In that study the supporting structure possessed 4% damping whereas the supported structure was characterized by 0.5% damping. Fig. 7 compares the apparent dynamic amplification factors obtained and proposed by Biggs with those predicted by Eq. (4) (for a damping ratio of 0.5%). The information summarized in Fig. 7 has been adapted from Biggs (1971) and therefore all quantities have been indicated using the original symbols proposed by the author. On the y-axis, A_e represents the peak equipment acceleration while A_{sn} is maximum acceleration in a mode *n* of the structure at the point of equipment support. On the x-axis, T_e indicates the equipment period of vibration while T_s stands for the natural period of the structure.
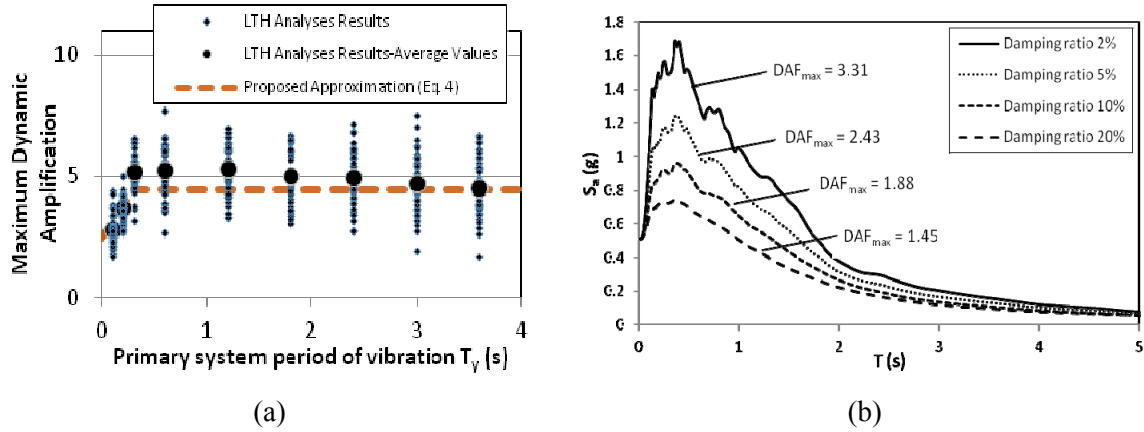
Fig. 6 (a) Apparent dynamic amplification factors obtained at 5% elastic damping from time-history analyses using 47 strong ground motions (Table 4) and SDOF supporting structures of varying period, and (b) Average ground response spectra constructed for different values of elastic damping using the same ground motion set.
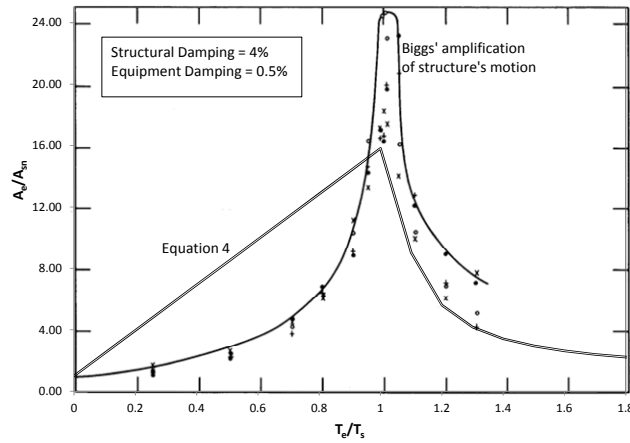

Fig. 7 Comparison of amplification of the structure's motion factors (i.e., apparent dynamic amplification factors) obtained at 0.5% elastic damping from Eq. 4 with those obtained via numerical analysis by Biggs

Encouragingly, Fig. 7 shows that Eq. (4) provides a good estimate of the peak dynamic amplification factors even though it does appear conservative in the short period range. Sullivan *et al.* (2013) had also observed such conservatism in their original proposal in the short period range but preferred to maintain the simplified equation, noting that the floor spectra are most influenced by the peak amplification factor.

The results of Fig.7 might suggest that the factors provided by Biggs (1971) should be applied in modern design. However, one difficulty with this is that Biggs did not provide generalized equations for dynamic amplification, and instead refers to figures (such as that in Fig. 7) that are used together with a series of relatively cumbersome equations applicable over different period

ranges. Another more important limitation of Biggs' procedure is that amplification factors were not provided for levels of elastic damping other than 0.5%. Finally, Biggs method does not account for the fact that the lower levels of a building tend to be relatively unfiltered, developing unexpectedly high floor accelerations, as will be illustrated later in this paper. Despite such criticisms, the work of Biggs (1971) has the merit of recognizing, as is recognized by the new procedure proposed in this paper, that floor response spectra should be constructed accounting for the effects of the elastic damping of the supported element and also for the influence of different modes of vibration.

4. Numerical investigation to verify the proposed approach

In order to verify the performance of the new approach for MDOF supporting structures, floor spectra obtained from the results of time-history analyses for five case study structures are compared with the floor spectra predicted by Eq. (1). It should be appreciated that the approach introduced in the previous section is not limited to specific supporting structure typologies. Nevertheless, RC walls are selected as case study structures since the floor accelerations in this type of systems tend to be high and strongly influenced by the actions of the higher modes.
This section is divided in two parts: firstly, the case study structures are described; secondly, details of the non-linear time-history modeling and analysis approach are provided.

4.1 Description of the case study RC wall structures

Fig. 8 presents the (part) plan and elevation of the regular case study structures considered. The lateral load resisting system in the buildings is provided by a series of walls in both directions. For the purposes of this study, only the response in the X-direction is examined since it is assumed that response in the X-direction will be independent of that in the Y-direction.

Material properties are typical of construction practice, with a concrete compressive strength, f_{ck}, of 25 MPa and reinforcement characteristic yield strength, f_{yk}, of 450 MPa. The structural layout is considered analogous to a hotel or apartment building in which RC walls act as both partitions and structural elements. This type of structural configuration was selected as it will tend

Table 2 Details of the RC wall structures

	Structure #1	Structure #2	Structure #3	Structure #4	Structure #5
Storeys	2	4	8	12	20
Wall length, L_w (m)	1	2	4	6	10
Wall thickness, t_w (m)	0.25	0.25	0.25	0.25	0.25
Seismic mass per wall (T/floor)	60	60	60	60	90
Wall base axial load (kN)	1178	2356	4704	7056	8800
Longitudinal reinforcement content, ρ (=$A_{sl}/L_w.t_w$)	0.05	0.05	0.05	0.05	0.05
Nominal flexural strength at wall base (kNm)	4490	8356	15686	23028	63070

Table 3 Periods of vibration (X-direction) for the case study structures

	Structure #1	Structure #2	Structure #3	Structure #4	Structure #5
First mode period of vibration, T_1 (s)	0.859	1	1.275	1.5	2.3
Second mode period of vibration, T_2 (s)	0.133	0.16	0.208	0.247	0.38
Third mode period of vibration, T_3 (s)	-	0.061	0.079	0.093	0.14

to be stiffer than other types of buildings and should be expected to have higher floor accelerations. Design of the structures was done in accordance with Eurocode 8 (CEN EC8 2004) for the type 1 spectrum with a ground acceleration of 0.4 g and soil type C. Details of the walls, including reinforcement contents and estimated base flexural strengths, are reported in Table 2. Note that owing to the large number of walls that were specified partly for architectural reasons (subdivision of apartments), it was found that design loads were satisfied with the use of minimum quantities of longitudinal reinforcement. Concerning structure number 5, it was also found that because of the large number of walls, an elastic response should be expected at the design earthquake intensity level. The reinforcement detailing for the walls is not shown here but it is assumed that good detailing would be provided in line with the EC8 recommendations to ensure ductile response under rare earthquake events.

In order to predict the roof level acceleration spectra in accordance with the new method previously described, the modal properties of the structures are required. As such, models of the RC wall structures were developed using elastic beam elements in Ruaumoko (Carr 2009) in which the cracked section stiffness of the walls was set as 50% of the un-cracked stiffness (which is approximate but agrees with EC8 recommendations) and seismic masses were lumped at floor levels. The first three periods of vibration obtained from the eigen-value analyses are reported below.

4.2 Linear time-history modeling and analysis approach

In order to investigate the elastic dynamic response of the case study structures, a series of linear time-history (LTH) analyses were conducted using two-dimensional lumped-plasticity models in Ruaumoko (Carr 2009). Elastic beam elements were used with elastic properties (with cracked section characteristics as per Section 4.1), lumped masses and concentrated gravity loads. A large displacement analysis regime was adopted and an integration time-step of 0.001s was used for the analyses. Elastic damping was modeled using a Rayleigh proportional damping model with 3% damping imposed on the first mode of vibration and 5% on the 2nd mode of vibration. A lower value of damping was placed on the 1st mode to a provide conservative estimation of demands, recognizing that actual damping values are uncertain and that damping components are likely to be affected by the quantity and type of non-structural elements (Welch *et al.* 2014a). Floors were assumed to behave as rigid diaphragms in-plane, fully flexible out of plane, and consequently nodes at the same level were constrained to move together. The columns and transverse walls (see Fig. 8) were assumed to provide no resistance in the X-direction. The foundations were assumed to behave rigidly and so were not modeled.

The same set of 47 accelerograms selected by Sullivan *et al.* (2013) have been used for the LTH analyses, uniformly scaled to match the Eurocode 8 type 1 response spectrum, for a soil type C, corresponding to very stiff soil conditions. A summary of the earthquake characteristics is

Table 4 characteristics of the accelerograms selecte4dfor the time-history analyses

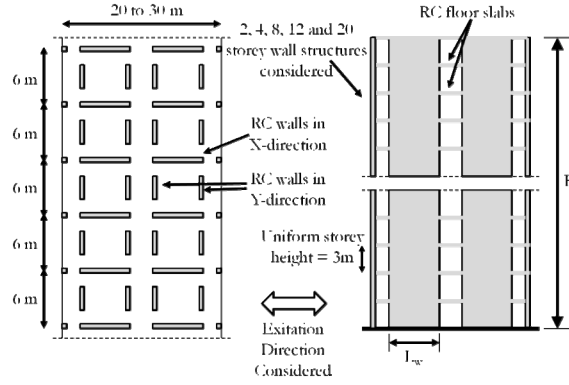| Earthquake Name	Date	M_w	Station	Epicentral Distance (km)	Scaling Factor	Significant Duration (s)
Adana	1998	6.3	ST549	30	4.84	10.74
Izmit	1999	7.6	ST772	20	1.59	12.88
Friuli aftershock	1976	6	ST33	9	12.35	15.4
Alkion	1981	6.6	ST122	19	1.44	10.54
Dinar	1995	6.4	ST271	8	1.88	8.7
Lazio Abruzzo aftershock	1984	5.5	ST152	24	1.7	10.75
Izmit aftershock	1999	5.8	ST3272	26	8.81	15.84
Northridge	1994	6.69	LA - Pico &Sentous	27.8	4.27	15.36
Kobe, Japan	1995	6.9	Shin-Osaka	19.1	2.18	13.32
Friuli, Italy	1976	6.5	Codroipo	33.3	6.18	18.7
Imperial Valley	1979	6.53	Delta	22	1.56	54.95
Chi-Chi, Taiwan	1999	6.2	TCU112	43.5	12.26	30.12
Chi-Chi, Taiwan	1999	6.2	CHY047	38.6	4.13	17.28
Coalinga	1983	6.36	Cantua Creek School	23.8	2.04	12.5
Chi-Chi, Taiwan	1999	6.3	CHY025	39.1	25.19	12.66
Chi-Chi, Taiwan	1999	6.3	CHY036	45.1	2.91	24.42
Chi-Chi, Taiwan	1999	6.3	TCU059	46.7	5.53	29.3
Chi-Chi, Taiwan	1999	6.3	TCU108	41.3	7.99	18.14
Chi-Chi, Taiwan	1999	6.3	TCU123	38.3	5.5	16.75
Morgan Hill	1984	6.19	Hollister Diff Array #3	26.4	6.27	20.9
Morgan Hill	1984	6.19	Hollister Diff Array #4	26.4	5.69	22.2
Morgan Hill	1984	6.19	Hollister Diff Array #5	26.4	6.25	21
Chalfant Valley	1986	6.19	Bishop -LADWP South St	14.4	2.62	11.17
Superstition Hills	1987	6.54	Brawley Airport	17	4.48	13
Superstition Hills	1987	6.54	Kornbloom Road (temp)	18.5	3.77	13.84
Superstition Hills	1987	6.54	Poe Road (temp)	11.2	1.73	13
Spitak, Armenia	1988	6.77	Gukasian	24	3.21	11.05
Loma Prieta	1989	6.93	Fremont - Emerson Court	39.7	3.91	14.12
Loma Prieta	1989	6.93	Gilroy Array #2	10.4	1.66	13.15
Loma Prieta	1989	6.93	Gilroy Array #4	13.8	1.88	17.87
Loma Prieta	1989	6.93	Halls Valley	30.2	4.43	13.65
Loma Prieta	1989	6.93	Hollister Diff. Array	24.5	1.7	10.07
Big Bear	1992	6.46	San Bernardino - E & Hosp.	34.2	4.48	25.87
Northridge-01	1994	6.69	Camarillo	34.8	3.71	12.66
Northridge-01	1994	6.69	Hollywood - Willoughby Ave	17.8	2.56	17.6
Northridge-01	1994	6.69	LA - Baldwin Hills	23.5	2.72	14.52
Northridge-01	1994	6.69	LA - Century City CC North	15.5	2.22	32.44
Denali, Alaska	2002	7.9	R109 (temp)	43	6.5	23.69
Chi-Chi, Taiwan	1999	7.62	TCU085	58	5.8	19.97
Chi-Chi, Taiwan	1999	7.62	TAP065	122	6.1	23.4
Chi-Chi, Taiwan	1999	7.62	KAU003	114	5.2	59.98
Darfield, NZ	2010	7.1	Rata Peats (RPZ)	93	13.4	24.36
Loma Prieta	1989	6.93	So. San Francisco, Sierra Pt.	63	7.2	12.14
Loma Prieta	1989	6.93	So. San Francisco, Sierra Pt.	63	6.8	9.54
Irpinia, Italy-01	1989	6.9	Auletta	10	7.9	18.96
Northridge-01	1994	6.69	Sandberg - Bald Mtn	42	6.2	15.92
Northridge-01	1994	6.69	Antelope Buttes	47	12.7	15.16

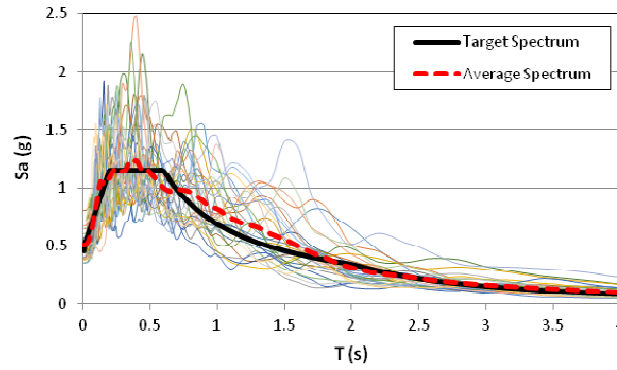Fig. 8 Illustration of the case study RC wall structure

Fig. 9 Acceleration response spectra at 5% elastic damping for the selected accelerograms, scaled to be spectrum compatible with the EC8 type 1 spectrum for soil type C and a PGA = 0.4 g

provided in Table 4, and the acceleration spectra of the records, uniformly scaled to match the EC8 spectrum at a PGA of 0.4 g, are presented in Fig. 9. The first seven records listed in Table 4 were taken from the RELUIS data base (www.reluis.it) and the next 40 records were selected from the PEER strong motion database (http://peer.berkeley.edu/nga/) except for the Darfield (New Zealand) record which was obtained from the New Zealand GeoNet Strong Motion Data ftp website (ftp://ftp.geonet.org.nz/strong/processed/Proc). Note that the set of records is characterized by an average magnitude of 6.6 and a distance from the epicenter of approximately 34 km. Note that the scale factors reported in Table 4 are for a design PGA of 0.4g.

5. Results of linear time-history analyses

The time history analyses were run for earthquake intensities proportional to peak ground accelerations varying between 0.1g and 0.4g, but in all cases the case study structures were modeled to respond elastically. This reflects the aims of this paper to extend the method of Sullivan *et al*. (2013) to elastically responding MDOF supporting systems and future research

should aim to extend the method to the case of inelastically responding MDOF systems. The reader must therefore bear in mind that the reliability of the proposed procedure to construct floor acceleration spectra being proposed can only be assumed if the supporting systems do not undergo inelastic deformations.

5.1 Peak floor accelerations

Fig. 10 presents the peak floor acceleration demands over the height of all five case study structures from time-history analyses using the accelerogram set from Table 4 (compatible with a PGA of 0.4g). The figure also includes the prediction obtained from the proposed procedure of Section 3.

It can be seen that the new simplified approach performs well as the shape and magnitude of the predicted peak floor accelerations matches the observed response well, with slightly conservative predictions made over upper levels and slightly non-conservative predictions for the lower levels of taller buildings.

Fig. 10 Variation of the peak floor acceleration (PFA) along the height of the building for (a) structure #1, (b) structure #2, (c) structure #3, (d) structure #4 and (e) structure #5. The PFA and height are normalized over PGA and total height of the building respectively

5.2 Floor response spectra obtained from the LTH analyses

Floor level response spectra can be obtained by first establishing the acceleration time-history recorded at the desired level during the LTH analyses and then using numerical techniques (see Chopra 2000) to establish the corresponding acceleration response spectra. Following this approach, the acceleration time-history record at each level has been used to construct floor response spectra associated for each level of all the case study structures listed in Table 2. This section presents the resulting floor spectra obtained for the 20-storey structure #5 (for which the effects of the higher modes are more pronounced) but readers should note that the results are representative of all the structures analyzed.

In order to highlight the manner in which elastic damping can affect floor spectra, Fig. 11 presents roof level response spectra at four different values of elastic damping. As expected, the acceleration intensities in the response spectra are extremely sensitive to the inherent damping selected. For instance, a larger damping implies that the curves scale down and vice versa (Fig. 11).
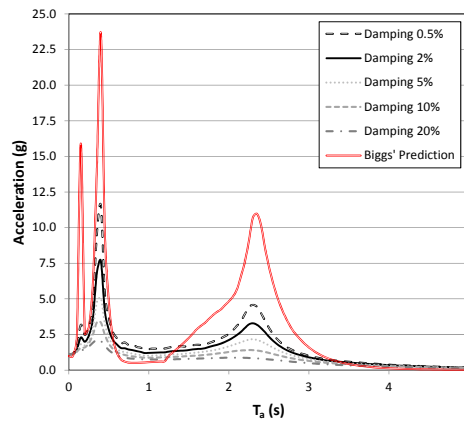

Fig. 11 Roof level response spectra predicted via time-history analyses of structure #5 subject to accelerograms compatible with the EC8 spectrum at a PGA = 0.4g.
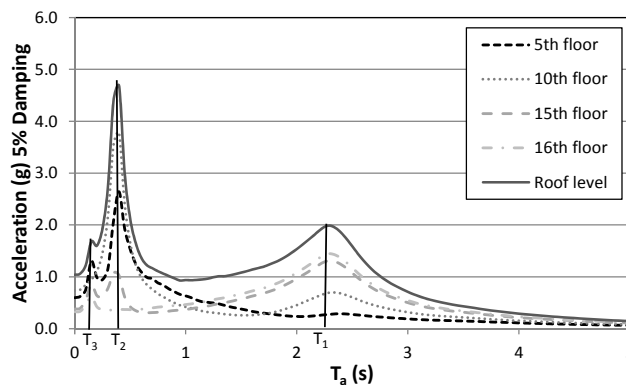

Fig. 12 Various level response spectra at 5% damping obtained from LTH analyses of structure #5 subject to accelerograms compatible with the EC8 spectrum at a PGA = 0.4 g
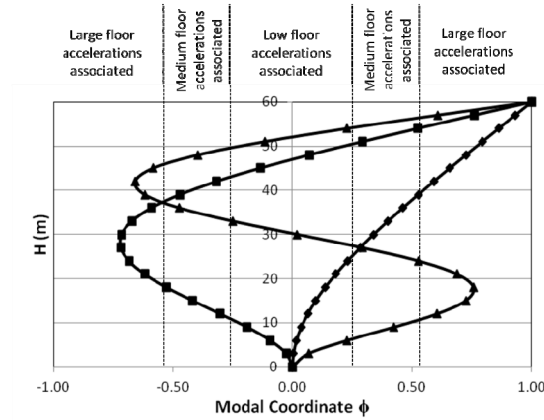
Fig. 13 Case study structure #5 first three mode shapes

Roughly speaking, doubling the damping corresponds to a 50% reduction in terms of acceleration demand. Fig. 11 also includes the predicted floor spectra obtained from Biggs approach. Note that the approach greatly overestimates spectral demands for all damping levels considered.

In addition to the component elastic damping, the response spectra are strongly influenced by the location (i.e. the floor) at which they are constructed. This is illustrated in Fig. 12 where 5% damped response spectra are plotted for various levels of the 20-storey case study structure. It can be seen that significant peaks occur in correspondence to the natural frequencies (periods) of the supporting structure, but these peaks are not present on all floors. This behaviour can be explained by considering the modal contributions at different levels and Fig. 13 presents the first three mode shapes obtained for the 20-storey case study #5.

The mode shapes shown in Fig. 13 can be examined to highlight the extent to which a specific mode is likely to contribute to the floor response spectra constructed at specific levels of the building. This is because the mode shapes are a direct representation of the associated peak floor accelerations. It can be seen from Fig. 13 that the 2nd mode has a nodal point at close to the 16[th]storey and consequently, this explains why the floor response spectra in Fig. 12 do not exhibit a significant peak at the 2nd mode period for floor 16. With this in mind, the mode shapes could be used to establish the location at which a strategic component, (e.g. mechanical equipment or similar) characterized by a specific period of vibration, should be positioned along the height of the structure. For instance, referring to case study structure #5, a component whose period of vibration is estimated to coincide with the second period of vibration of the main system (around 0.4 seconds), could be tentatively located at the 16th floor where little effects induced by the second mode of vibration are expected (Fig. 13).

For most structures, including case study #5, all of the main modes of vibration are likely to cause their highest acceleration demand at the roof level. At this location, even though the relative floor acceleration is large, it is reasonable to expect the effects of the mode 3 and above (or in general, the higher modes of vibration) to be negligible as the peak floor acceleration associated is lower than that of the second mode. Moreover, lower values of the DAF should be expected for accelerations associated with structures (or modes) characterized by periods of vibration shorter

than 0.3 seconds. This trend is confirmed by the analysis outcome, as the peak associated with the third mode is barely visible (as seen in Fig. 12). This points towards the possibility of a simplified modal approach that considers only the first two modes of vibration and this could be explored as part of future research.

5.3 Comparing the predicted and observed floor response spectra

Applying the procedure outlined in section 3 step by step, the spectra associated with the individual modes are constructed and subsequently combined using an SRSS approach. The resulting floor response spectra illustrated in this section are all associated with case study structure #5 and are all constructed for different levels of the supporting structure and for four different values of inherent damping (2%, 5%, 10% and 20% of the critical damping). The curves are constructed accounting for the effects of the first two or three modes. Even if not reported, the accuracy of the predictions obtained concerning the other case study structures is analogous to the one shown relatively to structure #5.

Figs. 14 to 17 present the floor spectra at the roof level, at the 16th floor, at the 5th floor and at the 1st floor respectively. At the roof level location, the peak floor acceleration reaches its highest value. At the 16th floor, a relatively important influence of the third mode is expected, while the effects of the second mode should substantially disappear. At the 5th floor, besides the contribution of both the second mode and the third mode (which is expected to be significant), the location along the height of the building is such that the filtering at some frequencies is limited and therefore the maximum between the modal combination and the ground spectrum is adopted (see discussion section 3.3). This is even more relevant at the 1st floor where it can be seen that the ground spectrum essentially dictates the predicted floor response spectrum.

As expected, while there is no need to account for the effects of the third mode for what regards the roof level (Fig. 13), the 16th floor response spectra in Fig. 15 present a relatively pronounced peak at the third period of vibration location, which would be missed if higher modes are not explicitly accounted for. On the contrary, and as would be expected from Fig. 13, there is no peak at the second period of vibration for floor 16 as its modal contribution at this level is low.

Concerning the 5th floor spectra, it can be observed in Fig. 16 that the peak floor acceleration is well predicted. Even though the effect of the third mode is relatively pronounced, the prediction obtained using the first two modes alone is satisfactory. This might at first appear puzzling considering that earlier in the paper and in other references, it has been emphasized that higher mode demands can be significant for floor spectra. As can be appreciated considering Fig. 13, the first three modes will dominate demands on upper levels while higher modes will contribute more over lower levels. However, for reasons explained in Section 3.2, limited filtering occurs over these lower levels and hence even if all modes of vibration in a 20-storey structure were included, floor spectra would not necessarily be well predicted at all frequencies. For this reason, the recommendation made in Section 3 was to adopt the maximum between the ground spectrum and the modal combination (for the first three modes), and this appears to work well as seen in Fig. 16. This is even more evident at the 1st floor as shown in Fig. 17 where it is seen that the ground level spectra provide a good indication of the first floor spectra, confirming that filtering is not significant over the lower storeys.

Overall, the results illustrated in Figs. 14 to 17 demonstrate that the new approach provides an effective means of predicting floor spectra since the spectral peaks and the general shape of the
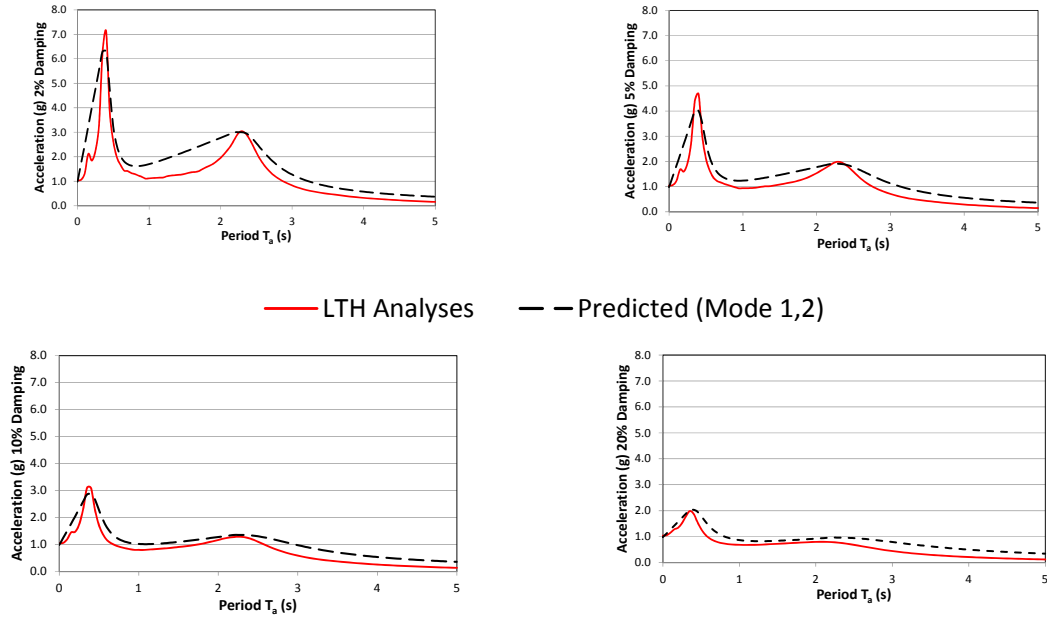
Fig. 14 Comparison of roof level spectra at 2%, 5%, 10% and 20% damping predicted by Eq. (1) with those obtained from LTH analyses of the 20-storey case study structure using the accelerograms listed in Table 4
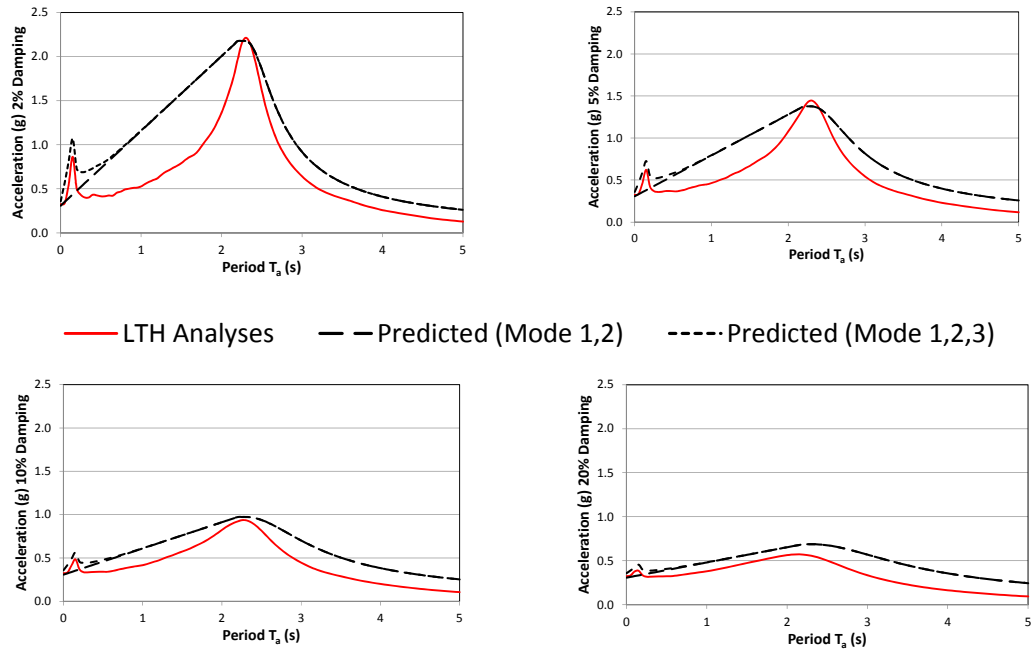

Fig. 15 Comparison of 16th floor spectra at 2%, 5%, 10% and 20% damping predicted by Eq. (1) with those obtained from LTH analyses of the case study structure using the accelerograms listed in Table 4
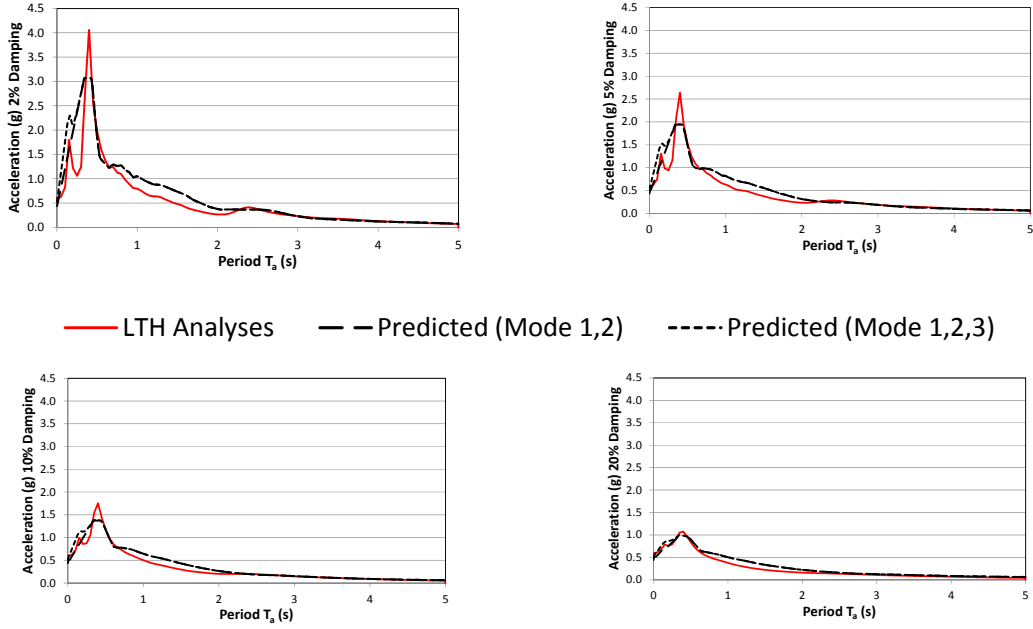
Fig. 16 Comparison of 5th floor spectra at 2%, 5%, 10% and 20% damping predicted by Eq. (1) with those from LTH analyses of the case study structure using the accelerograms listed in Table 4
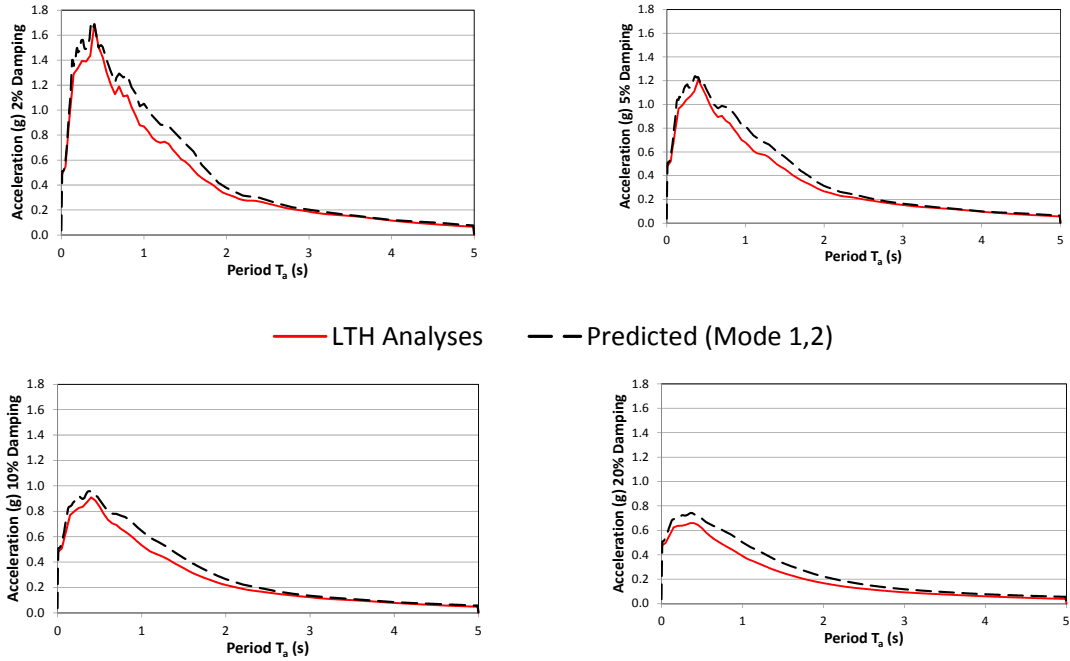

Fig. 17 Comparison of 1st floor spectra at 2%, 5%, 10% and 20% damping predicted by Eq. (1) with those from LTH analyses of the case study structure using the accelerograms listed in Table 4

spectra are well predicted, for different levels of damping, at different locations of the case study structures. One should note that as the earthquake intensity is varied (either increased or decreased) the floor spectra are still well predicted (noting that this work is limited to the case of elastic response). One aspect that should be pointed out is that in general, the peaks of the spectra are slightly underestimated, particularly for low levels of inherent damping. This suggests that minor adjustment of Eq. (4) for low damping level could be made, as part of future work.

6. Conclusions

Recently, a new procedure was successfully developed and tested by Sullivan *et al.* (2013) for the simplified construction of floor spectra, at various levels of elastic damping, atop single-degree-of-freedom structures. This paper has extended the methodology to multi-degree-of-freedom (MDOF) supporting systems responding in the elastic range. The new method first scales floor acceleration components obtained from modal analyses by empirical dynamic amplification factors that are set as a function of the period of the supporting structure and the period and elastic damping of the supported component. The acceleration demands for each mode are then combined using a SRSS approach to give the predicted floor spectra over upper levels. Over the lower levels of the building it has been recognized that the arriving ground motion will undergo little filtering and subsequently, floor spectra are set as the maximum of the ground level response spectrum and the floor spectra obtained from the modal approach advocated for the upper storeys.

The new procedure has been tested numerically by comparing predictions with floor spectra obtained from time-history analyses of RC wall structures of 2- to 20-storeys in height using a set of 47 recorded ground motions. Results demonstrate that the method performs well for MDOF systems responding in the elastic range. While the procedure is currently limited to prediction of floor spectra in the elastic range, this procedure could still be particularly useful for engineers interested in controlling damage at the serviceability limit state for which elastic response of the supporting structure would typically be expected. Nevertheless, future research should further develop the approach to permit the prediction of floor spectra in MDOF systems that respond in the inelastic range.

References

Biggs, J.M. (1971), "Seismic response spectra for equipment design in nuclear power plants", *Proceeding of the 1st International Conference Struct. Mech. Rreact. Techn.*, Berlin, Paper K4/7.

Carr, A.J. (2009), Ruaumoko3D – A program for Inelastic Time-History Analysis, Department of Civil Engineering, University of Canterbury, New Zealand.

CEN EC8 (2004), *Eurocode 8 – Design Provisions for Earthquake Resistant Structures*, EN-1998-1:2004: E, Comite Europeen de Normalization, Brussels, Belgium.

Chopra, A.K. (2000), "Dynamics of structures", Pearson Education, USA.

Garcia, R., Sullivan T.J. and Della Corte, G. (2010), "Development of a displacement-based design method for steel frame-RC wall buildings", *J. Earthq. Eng.*, **14**(2), 252-277.

Igusa, T. and Der Kiureghian, A. (1985), "Generation of floor response spectra including oscillator-structure interaction", *Earthq. Eng. Struct. Dyn.*, **13**(5), 661-676.

Kumari, R. and Gupta V.K. (2007), "A modal combination rule for peak floor accelerations in multistoried buildings", *ISET J. Earthq. Tech.*, **44**(1), 213-231.

Maley, T.J., Sullivan, T.J. and Della Corte, G. (2010), "Development of a displacement-based design method for steel dual systems with buckling-restrained braces and moment resisting frames", *J. Earthq. Eng.*, **14**(1), 106-140.

Menon, A. and Magenes, G. (2008), *Out-of-plane Seismic Response of Unreinforced Masonry Definition of Seismic Input*, Research Report ROSE – 2008/04, IUSS Press, Pavia, Italy, 269 pages.

Mondal, G. and Jain, S.K. (2005), "Design of non-structural elements for buildings: A review of codal provisions", *Indian Concrete J.*, **79**(8), 22-28.

Oropeza, M., Favez, P. and Lestuzzi, P. (2010), "Seismic response of nonstructural components in case of nonlinear structures based on floor response spectra method", *Bull. Earthq. Eng.*, **8**(2), 387-400.

Pennucci, D., Sullivan, T.J. and Calvi, G.M. (2011), *Performance-Based Seismic Design of Tall RC Wall Buildings*, Research Report ROSE2011/02, IUSS Press, Pavia, Italy, 319pages.

Priestley, M.J.N., Calvi, G.M. and Kowalsky, M.J. (2007), "Direct displacement-based seismic design", IUSS Press, Pavia, Italy, 720 pages.

Rodriguez, M.E., Restrepo, J.I. and Carr, A.J. (2002), "Earthquake-induced floor horizontal accelerations in buildings", *Earthq. Eng. Struct. Dyn.*, **31**, 693-718.

Singh, M.P. (1980), "Seismic design input for secondary systems", *J. Struct. Div. ASCE*, **106,** 505-517.

Sullivan, T.J. (2011), "An energy factor method for the displacement-based seismic design of RC wall structures", *J. Earthq. Eng.*, **7**(15), 1083-1116.

Sullivan, T.J. (2013), "Highlighting differences between force-based and displacement-based design solutions for RC frame structures", *Struct. Eng. Int.*, **23**(2), 122-131.

Sullivan, T.J., Calvi, P.M. and Nascimbene, R. (2013), "Towards improved floor spectra estimates for seismic design", *Earthq. Struct.*, **4**(1), 109-132..

Taghavi, S. and Miranda, E. (2006), "Seismic demand assessment on acceleration-sensitive building non-structural components", *Proceedings of the 8th National Conference on Earthquake Engineering*, San Francisco, California, USA, April.

Vanmarcke, E.H. (1977), "A simplified procedure for predicting amplified response spectra and equipment response", *Proceeding of the 6th World Conference Earthquake Engineering* III New Delhi, India, 3323-3327.

Villaverde, R. (2004), "Seismic analysis and design of non-structural elements in Earthquake engineering from engineering seismology to performance-based design", (Eds) Y. Bozorgnia, V.V. Bertero, CRC Press, 19-48.

Welch, D.P., Sullivan, T.J. and Calvi, G.M. (2014), "Developing direct displacement-based procedures for simplified loss assessment in performance-based earthquake engineering", *J. Earthq. Eng.*, **18**(2), 290-322

Welch D.P., Sullivan T.J. and Filiatrault, A. (2014a), "Equivalent structural damping of drift-sensitive nonstructural building components", *Proceedings of the 10th National Conference in Earthquake Engineering*, Earthquake Engineering Research Institute, Anchorage, Alaska, USA, July.

SA